

LES-VMS SIMULATIONS OF THERMALLY STRATIFIED TURBULENT WAKES BEHIND TOWED AND AUTO-PROPELLED AXISYMMETRICAL BODY

B. Sainte-Rose *
LEMMA USA, inc.
Houston, TX, 77008, USA
Email: bruno.sainte-rose@lemma-ing.com

X. Lenhardt
DGA Techniques Navales
Toulon, 83050, France
Email: xavier.lenhardt@dga.defense.gouv.fr

O. Allain
LEMMA
Sophia-Antipolis, 06140, France
Email: olivier.allain@lemma-ing.com

M. Berton
LEMMA
Toulouse, 31600, France
Email: mikael.berton@lemma-ing.com

A. Dervieux
LEMMA
Sophia-Antipolis, 06140, France
Email: alain.dervieux@inria.fr

ABSTRACT

Numerical simulations of close and far wakes behind an axisymmetrical body in a stratified medium are carried out using a Large Eddy Simulation - Variational Multi Scale approach to model turbulence. Towed and auto-propelled flow regimes are scrutinized and compared. The characteristic parameters of the flow are $Pr = 7$, $Re = 10000$ based on the diameter of the cylinder and $F = 25$. Realistic results are obtained for the towed case where the so-called three-dimensional (3D), non-equilibrium (NEQ) and quasi two-dimensional (Q2D) regimes are exhibited with very good agreement with experimental and theoretical findings of the literature. In addition, the effect of auto-propulsion on the flow dynamics is reproduced in a satisfying manner.

INTRODUCTION

Context

The understanding of far turbulent wakes in thermally stratified water is of prime interest for submarine engineers concerned with both hydrodynamic and acoustic stealths. Indeed, the massive separation and the resulting turbulent flow downstream of the device generate both velocity and temperature fluctuations which to turbulent kinetic energy / dissipation and thermal dissipation. Such characteristics of

the flowfield can be measured by detection devices. In addition, the variations of the fluid's density can be identified in the reflected signal captured by a sonar. Hence, the objective of submarine engineers is to understand the time-evolution of such quantities in order to establish the influence of parameters such as Reynolds and Prandtl numbers, angle of attack, propulsion, asymmetry, appendages... Their goal is to find a relation between the variations of the measured quantities and the properties of the device (nature of the object, distance, cruising regime, size...) in order to qualify the signals obtained for detection purposes. However, such flows are tedious to accurately analyse on simple theoretical grounds because of non linear phenomena such as turbulence and also because of the complexity of the geometries considered. Moreover, reproducing such wakes at a reasonable scale is very demanding experimentally and the subsequent measurements only give access to a limited number of data too scarce to allow an accurate description of the flow. On the other hand, thanks to the increasing reliability of Computational Fluid Dynamic approaches and the growth of High Performance Computing, numerical simulations of such phenomena are now utilized to tackle such stringent issues. These methods give the engineers an affordable and trustworthy alternative to costly and time-consuming experimental campaigns. Thus, the understanding of turbulent far wakes is made possible thanks to a joint effort between experimental, theoretical and numerical approaches.

*Address all correspondence to this author.

State of the art

The effect of thermal stratification and gravity in the close wake behind a towed sphere has been thoroughly investigated experimentally by Bonneton *et al.* (1996). These investigations concern low Reynolds numbers and weak stratification (via the internal froude number $F = NU_0/R$ where N is the Brunt-Vaisala frequency and is defined as $N^2 = -g\partial_Y\rho/\rho_0$ where Y denotes the vertical direction and ρ_0 is the density in the center of the domain). Concerning far wakes, the effect of gravity has been proven to result into specific flow patterns ultimately leading to bi-dimensional shapes as evidenced by Spedding *et al.* (1996). Further investigations were conducted on different body shapes to educe universal laws and address the influence of propulsion (with or without momentum) in the following papers (Meunier & Spedding (2004); Meunier *et al.* (2006); Meunier & Spedding (2006)). The influence of auto-propulsion (without momentum stratified wakes) has been addressed theoretically by Lin & Pao (1979).

Numerically, the close stratified wakes behind several types of bodies have been commonly simulated. At first, these computations were conducted using cost-effective Reynolds Averaged Navier Stokes (RANS) methods in (Hanazaki (1988); Lin *et al.* (1992)) where the whole turbulent scales spectrum is modelled and the results obtained are time averaged. Nowadays, the increasing computational power allows the use of Large Eddy Simulation (LES) to solve the flow around bluff bodies like in Dommermuth *et al.* (2002). When it comes to simulating the far wakes, the most convenient way is to assume periodicity in the streamwise direction and conduct a temporal development. This method has indeed been successfully used by Gourlay *et al.* (2001) with an initial flowfield deduced from statistical properties. More recently, such an approach has also been employed by for wakes with a moderate excess momentum in (de Stadler & Sarkar (2011, 2012)). However, such methods are irrelevant when it comes to take into account shaped geometries. To cope with this limitation Pasquetti (2011) suggests to carry out a preliminary close wake simulation which constitutes an ad-hoc initial condition for the temporal development.

Methodology and outline of the paper

In the current work, a numerical study of the far wakes behind a towed and auto-propelled axisymmetrical body is addressed. The simulations are run in two steps following the approach introduced by Pasquetti (2011). First the close wake behind the body is simulated to set appropriate initial conditions for the far wake development. Then, the far wake is simulated assuming periodic conditions in the streamwise direction and one scrutinizes its evolution in time for a duration corresponding to a length of more than a thousand diameters of the body. This methodology is summarized in figure 1 (a third part corresponds to the post-processing).

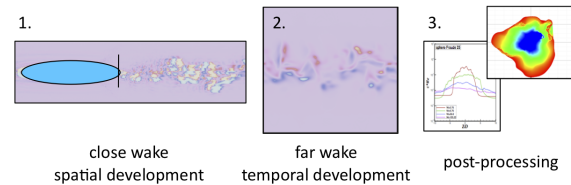


Figure 1. Schematic view of the study

Thus, this paper is organized as follows. In the first part, we present the physical models and numerical approaches handled by the ANANAS code used for our simulations. In a second part, the test case used for the close wake spatial development is introduced and the results of the computations are analyzed. In a third part, the temporal development simulations are presented and the results are discussed.

PHYSICAL MODELLING AND NUMERICAL METHODS

The computations are run using ANANAS, LEMMA's commercial code which solves the incompressible balance equations for mass and momentum. This code has proven its efficiency to solve numerous problems in hydrodynamics such as free-surface flows (Lesage *et al.* (2007); Guegan *et al.* (2010)) and turbulence around offshore platforms Simivas *et al.* (2006). The code uses tetrahedral elements and is based on a mixed finite volume - finite element method. Time integration is carried out using a third order explicit scheme while space integration is handled with the V6 high order scheme introduced by Koobus *et al.* (2008) which yields to sixth order for uniform mesh spacing. Turbulence is modelled thanks to Large Eddy Simulation Variational Multi-Scale model introduced by Hughes *et al.* (2000) which enables the resolution of turbulent structures scaling down to the mesh size.

Propulsion is handled with an actuator disk method such as the one detailed by Jacquin (2007), which provides a source term to the momentum equation. In the current approach, the auto-propelled regime is obtained when the thrust imposed through the actuator disk method balances the average drag obtained on the body. In figure 2, the equilibrium between non-dimensionnal drag and thrust during the simulation of the auto-propelled close wake is displayed.

CLOSE WAKE SIMULATION

Presentation of the numerical test case

Geometry of the problem The device studied, illustrated in figure 3 is composed of a half sphere of diameter D extended by a $3D$ long cylinder and a truncated cone (45° at the tip). The parameters of the flow are the Prandtl, Reynolds and internal Froude numbers that we take equal to $Pr = \kappa/\nu = 7$ where κ is the thermal diffusivity and ν the kinematic viscos-

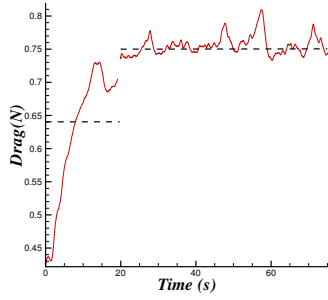


Figure 2. Equilibrium between non dimensionnall drag and thrust during the auto-propelled close wake simulation

ity, $Re = U_0 D / \nu = 10000$ and $F = 25$ (which gives a Brunt-Vaisala frequency N of $25s^{-1}$). The diameter of the propeller is equal to $0.7D$ (input for the actuator disk approach not detailed in this paper see Jacquin (2007)).

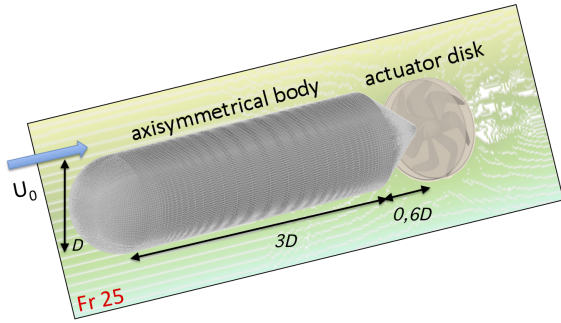


Figure 3. Sketch and dimensions of the close wake case

Computational domain and grids For the spatial development simulation, the domain considered is a rectangular parallelepiped which dimensions ($L_x = 41D$, $L_y = 8D$, $L_z = 8D$) enable us to capture $30.5D$ of turbulent wake. The mesh is fully structured as illustrated in figure 4 and its main characteristics are summarized in table 1 (the height of the first cell near the wall is given). It must be noticed that in the wake region (identified with a pink rectangle in the figure) the mesh is uniform so we can expect high order space resolution in this area of the computational domain.

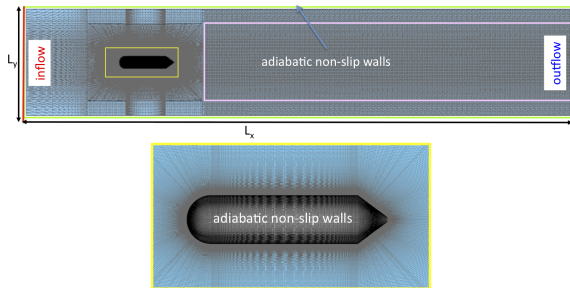


Figure 4. Mesh in the mid-span section (top), zoom on the mesh around the body (bottom)

Concerning the boundary conditions, a linearly strat-

Table 1. Mesh spacing and number of elements

Points count	$y_0^+, y_0/D$	Δ in the wake
5, 100, 000	0, 4; 0, 001	$\Delta x = \Delta y = \Delta z = 0, 075D$

ified flow at velocity U_0 is imposed in the inflow section and hydrostatic pressure in the outlet section. On the horizontal and lateral walls, adiabatic slip conditions are taken while no-slip adiabatic wall is assumed on the body.

Parameters of the computations The timestep used in the computations so as to verify $CFL_{max} = 0.5$ is equal to $\delta t = D/U_0 \times 0.002$. The decentering parameter varies from 1 near the wall to 0.3 in the wake. The simulation covers a physical time of $45D/U_0$ so that the wake that will be used as an initial condition to the temporal development is fully established.

Results and discussion

Instantaneous flowfields Visualisation of instantaneous flowfields are provided in figure 5 where Q criterion iso-surfaces are drawn to highlight the coherent turbulent structures downstream of the device for both regimes. Q criterion writes as :

$$Q = \frac{1}{2}(\Omega : \Omega - S : S) \quad (1)$$

where

$$\Omega = \frac{1}{2} [\nabla u - (\nabla u)^t] \text{ et } S = \frac{1}{2} [\nabla u + (\nabla u)^t]. \quad (2)$$

The results obtained in that figure are very realistic

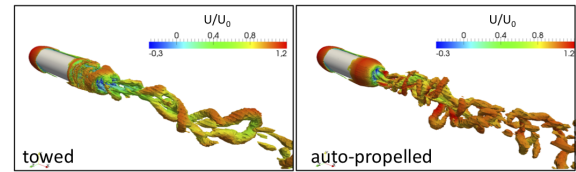


Figure 5. Q criterion iso-surfaces $Q(D/U_0)^2 = 0.1$ colored by the non-dimensional streamwise velocity

and the influence of propulsion on the flow dynamics is clearly highlighted. In the towed case the flow separates at the base of the cone and reattaches approximately three diameters downstream. At separation the flow is rather axisymmetrical and then becomes tri-dimensionnall further in the recirculation region and at reattachment where the turbulent structures start to

stretch and align with the flow. On the other hand, the nature of the flow is drastically changed by propulsion by sucking in the separating flow towards the axis of the body and giving birth to smaller and more numerous vortices downstream of the propeller, the actuator disk source term providing both streamwise and tangential contributions to the flow's momentum. In addition, the corresponding structures are smaller and display a higher streamwise velocity than for the towed case.

The effect of the turbulent mixing induced by the wake on the thermal flow field is shown in figure 6 where temperature iso-contours are drawn in the midspan section. In this figure, one can identify the turbulent structures dealt with in the previous paragraph which means that convection effects are predominant in this phase. Moreover, this figure evidences that the auto-propelled wake has a greater extension than the towed case.

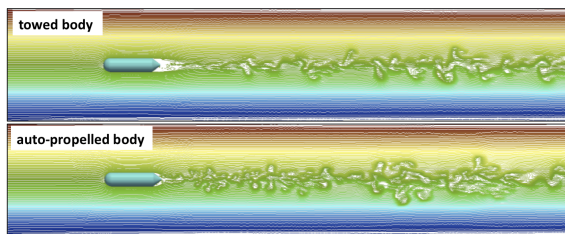


Figure 6. Instantaneous temperature fields in the mid-span section, from blue (low) to red (high)

Averaged flowfields The results of our simulations are averaged during a physical time Δt verifying $\Delta t U_0/D = 15$. The averaged streamlines and velocity flowfields are displayed in figure 7 for the region near the cone. In this figure the previous remarks concerning the shape of the separated region are confirmed: in the towed case a large separation with a fluidic reattachment is displayed; in the auto-propelled regime, the flow is vacuumed towards the tip of the cone *i. e.* upstream of the actuator disk. The propulsive effect of the actuator disk can be spotted with the occurrence of higher velocity regions evidenced with the $U = U_0$ iso-contours in the peripheral and the occurrence of a lower velocity lip which corresponds to the tip of the propeller. The $U = U_0$ iso-contours also demonstrate a greater wake extension for the auto-propelled case. The streamwise velocity profiles are drawn vertically at several locations in the x direction and along the x axis in figure 8 starting at $x = 0$ on the base of the cone: at $x/D = 0.5$ (solid lines), the suction effect of the propeller is evidenced by reducing the size of the recirculation bubble leading to greater negative values of the streamwise velocity; at $x/D = 4$ (dashed lines), the deficit for the towed case is four times higher than the auto-propelled; at $x/D = 20$ (dash dotted lines) the deficit is still 30% smaller for the auto-propelled case.

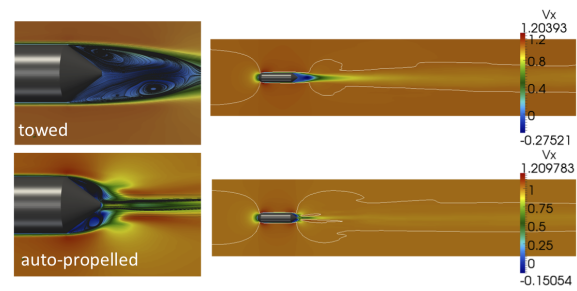


Figure 7. Averaged streamlines in the mid-span and streamwise velocity flowfield in the separation region (left); streamwise velocity and $U = U_0$ iso-contour in white (right)

One can also notice in that figure that the deficit observed for the close wake in the auto-propelled regime collapses much faster than in the towed regime if we look at the profile along the x axis ($x/D \approx 5$ against $x/D \approx 20$).

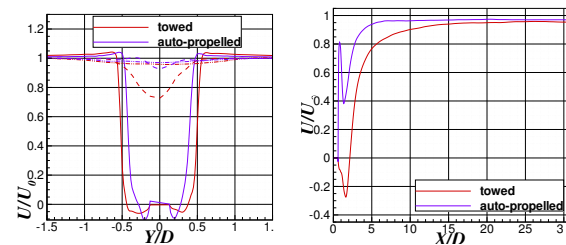


Figure 8. Averaged non-dimensional streamwise velocity profiles in several streamwise locations (vertically) (left) and averaged streamwise velocity along the X axis (right)

FAR WAKE SIMULATIONS

Presentation of the numerical test case

Computational domain and initial flowfield For the temporal development, the dimensions ($L_X = 36D$, $L_Y = 8D$, $L_Z = 24D$.) are taken so as to be able to simulate the large vertically flattened vortices encountered in the far wake (Y being the vertical direction) so the domain has to be enlarged compared to the close wake study. The mesh is uniform with $\Delta/D = 0.15$ in terms of mesh spacing which leads to a mesh size of $2,2M$ points. This new domain is centered on $x/D = 13$ where x is the distance to the base of the cone.

Since periodicity is assumed in the x direction, several steps are required to build an accurate initial flowfield. First the close wake flow field is projected on a domain of $18D$ in length between $x/D = 4$ and $x/D = 22$. Then a symmetry is operated to obtain the flowfields on the left and right domains. The new streamwise velocity is obtained by subtracting the bulk velocity U_0 . Then, the flowfield is extended in the spanwise directions assuming a zero velocity flowfield and a temperature flowfield with the initial

linear vertical stratification. The sequence of operations along with the dimensions and mesh are displayed in figure 9. Moreover, slip adiabatic conditions are assumed in the horizontal and lateral boundaries. The rationale behind the choice of such an approach and dimensions to initialize the flowfield is discussed by Pasquetti (2011).

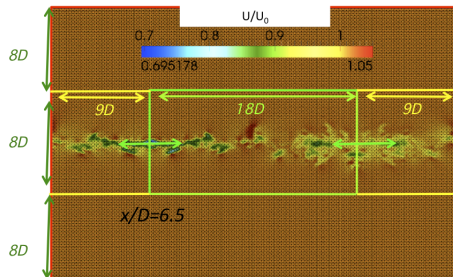


Figure 9. Dimensions of the mesh and initial conditions projected on the new mesh (limits in red), close wake domain limits (in green), reflected domain limits (in yellow)

The simulations are run during a physical time of $\Delta t = 100/N$, the decentering parameter is equal to 0.2 and the time step varies from $\delta t U_0/D = 0.025$ to $\delta t U_0/D = 0.25$ since the velocity fluctuations collapse along the temporal development.

Results and discussion

Evolution of the velocity deficit The evolution of the non-dimensional velocity deficit $\Delta U/U_0$ versus Nt is reproduced for both regimes in figure 10 where t is taken equal to $t_{sim} + t_0$ where t_0 corresponds to the time of the initial condition *i.e* $t_0 U_0/D = 13$ and t_{sim} the physical time of the simulation. In this figure a comparison with theoretical laws (Lin & Pao (1979); Spedding *et al.* (1996); Meunier & Spedding (2004)) and experimental ones (Meunier & Spedding (2006); Meunier *et al.* (2006)) giving the decay rate of the velocity deficit is provided. For the towed case the three phases (corresponding to three decaying rates) so-called three-dimensional (3D), non-equilibrium (NEQ) and quasi two-dimensional (Q2D) are identified in agreement with the work of Spedding Spedding *et al.* (1996). In the auto-propelled case, the initial decay is much more important and slows down at the end but leads to one decade difference compared to the towed case. This behaviour is in agreement with the work of Meunier & Spedding (2006).

Instantaneous flowfields To understand the mechanisms involved in the two different scenarii that arise in terms of velocity deficit decay, one can analyse the evolution of the turbulent structures in the far wake along the simulation. In figure 11 the vertical component of the vorticity is drawn for

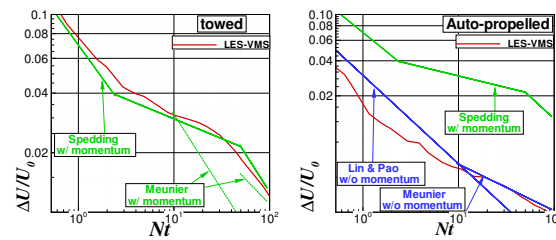


Figure 10. Velocity deficit vs Nt and comparison with other studies

$Nt = 0.76, 6.76, 29.2, 100.5$ (the maximum non-dimensional vorticity $|\omega_y D/U_0|$ in the colormaps are 0.6, 0.2, 0.04, 0.01). The results of the experiments of Meunier & Spedding (2006) for greater Nt numbers are also displayed in this figure (maximum non-dimensional vorticity equal to 0.1). In this figure we can observe that we obtain qualitatively the same behaviour for both conditions. In the towed case the expansion of the wake is slow and the turbulent structures progressively combine into large scale structures. For the auto-propelled regime, the wake expands faster (so as the deficit decay) at the beginning, the vortices are smaller and have less kinetic energy than in the towed case. However, at the end of the temporal development, it appears that the shape of the vortices are less sensitive to the gravity effects which explains the slow down in the decay highlighted in figure 10.

For the same times and with the same colormap for the vorticity, spanwise vorticity and temperature are drawn in figure 12. This figure allows us to analyze the structure of the vortices in the lateral direction and the influence on temperature. In the towed case the structures get organized into parallel flattened shape structures. In the auto-propelled case, the flow remains 3D, and the dynamics of the vortices is quite similar. In terms of temperature it appears that the stratification is recovered fast in this direction, partly due to higher diffusive effects.

CONCLUSIONS AND FUTURE WORK

In this study, an approach based on the combination of spatial and temporal developments to address close and far wakes behind an axisymmetric elongated body is successfully applied. In addition, auto-propelled flow regimes are considered and allow a quantitative evidencing of the differences with towed conditions. As a matter of fact, a faster decay of the wake deficit is evidenced in auto-propelled conditions in agreement with previous theoretical and experimental studies, the influence of the smaller structures which are more dissipative are highlighted in the instantaneous flowfields. Future work would be to apply this method to a more realistic geometry and Reynolds number and to scrutinize the influence of the propulsion model.

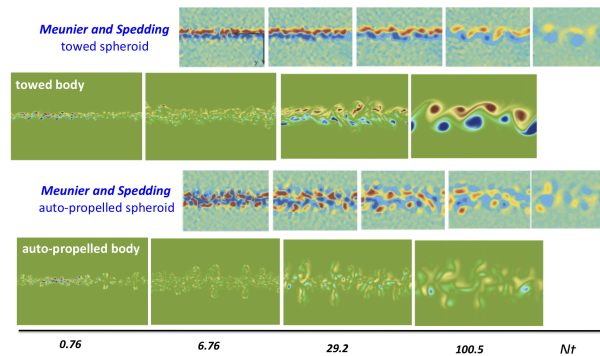


Figure 11. Instantaneous vertical vorticity in the center horizontal section and comparison with Meunier & Spedding (2006)

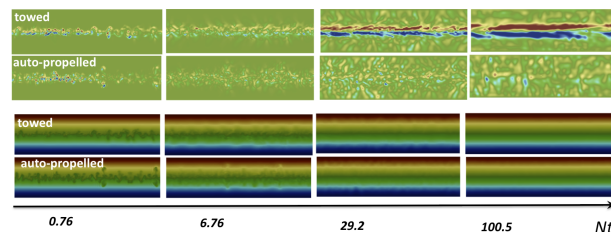


Figure 12. Instantaneous spanwise vorticity (top) and temperature in the mid-span section (bottom)

ACKNOWLEDGMENT

The authors gratefully acknowledge R. Pasquetti (Universite de Nice) for his help in implementing the method and for fruitful discussions on the physics of stratified wakes.

REFERENCES

- Bonneton, P., Chomaz, J.M., Hopfinger, E. & Perrier, M. 1996 The structure of the turbulent wake and the random internal wave field generated by a moving sphere in a stratified fluid. *Dynamics of Atmospheres and Oceans* **23**, 299–308.
- Dommermuth, D. G., Rotman, J. W., Innis, G. E. & Novikov, E. A. 2002 Numerical simulation of the wake of a towed sphere in a weakly stratified fluid. *J. Fluid Mech.* **473**, 83–101.
- Gourlay, M. J., Arendt, S. C., Fritts, D. C. & Werne, J. 2001 Numerical modeling of initially turbulent wakes with net momentum. *Phys. Fluids* **13** (12), 3783–3802.
- Guegan, D., Allain, O., Dervieux, A. & Alauzet, F. 2010 An L_∞ – L_p mesh-adaptive method for computing unsteady bi-fluid flows. *Int. J. Num. Meth. Eng.* **84** (11), 1376–1406.
- Hanazaki, H. 1988 A numerical study of three-dimensional stratified flow past a sphere. *J. Fluid Mech.* **192**, 393–419.
- Hughes, T.J.R., Mazzei, L. & Jansen, K.E. 2000 Large eddy simulation and the variational multi-scale method. *Comput. Vis. Sci.* **3**, 47–59.
- Jacquin, E. 2007 Navire autopropulsé en manœuvre : simulation numérique et optimisation des performances hydrodynamiques. PhD thesis, Ecole Centrale de Nantes.
- Koobus, B., Wornom, S., Camarri, S., Salvetti, M.V. & Dervieux, A. 2008 Nonlinear V6 schemes for compressible flows. *Tech. Rep.* RR-6433. INRIA.
- Lesage, A. C., Allain, O. & Dervieux, A. 2007 On level set modelling of bi-fluid capillary flow. *Int. J. Num. Meth. Fluids* **53** (8), 1297–1314.
- Lin, J.T. & Pao, Y.H. 1979 Wakes in stratified fluids. *Ann. Rev. Fluid Mech.* **11**, 317–338.
- Lin, Q., Lindberg, W., Boyer, D. L. & Fernando, H. J. S. 1992 Stratified flow past a sphere. *J. Fluid Mech.* **240**, 315–354.
- Meunier, P., Diamessis, P. & Spedding, G. R. 2006 Self-preservation in stratified momentum wakes. *Phys. Fluids* **18** (10).
- Meunier, P. & Spedding, G. R. 2004 A loss of memory in stratified momentum wakes. *Phys. Fluids* **16** (2), 298–305.
- Meunier, P. & Spedding, G. R. 2006 Stratified propelled wakes. *J. Fluid Mech.* **552**, 229–256.
- Pasquetti, R. 2011 Temporal / spatial simulation of the stratified far wake of a sphere. *Comp. Fluids* **40**, 179–187.
- Sirnivas, S., Wornom, S., Dervieux, A., Koobus, B. & Allain, O. 2006 A study of les models for the simulation of a turbulent flow around a truss spar geometry, omae2006-92355. *Proceedings of OMAE 2006*.
- Spedding, G. R., Browand, F. K. & Fincham, A. M. 1996 Vertical structure in stratified wakes with high initial froude number. *J. Fluid Mech.* **23**, 171–182.
- de Stadler, M. B. & Sarkar, S. 2011 Self-propelled wakes at different Froude numbers in a stratified fluid. In *TSFP 7, Ottawa, Canada*.
- de Stadler, M. B. & Sarkar, S. 2012 Simulation of a propelled wake with moderate excess momentum in a stratified fluid. *J. Fluid Mech.* **692**, 28.